JOURNAL OF GEOPHYSICAL RESEARCH, VOL. 99, NO. A10, PAGES 19,393–19,402, OCTOBER 1, 1994

Method for confining the magnetic field of the cross-tail current inside the magnetopause

T. Sotirelis, N. A. Tsyganenko, and D. P. Stern

Laboratory for Extraterrestrial Physics, NASA Goddard Space Flight Center, Greenbelt, Maryland

Abstract. A method is presented for analytically representing the magnetic field due to the cross-tail current and its closure on the magnetopause. It is an extension of a method used by Tsyganenko (1989b) to confine the dipole field inside an ellipsoidal magnetopause using a scalar potential. Given a model of the cross-tail current, the implied net magnetic field is obtained by adding to the cross-tail current field a potential field $\mathbf{B} = -\nabla\gamma$, which makes all field lines divide into two disjoint groups, separated by the magnetopause (i.e., the combined field is made to have zero normal component with the magnetopause). The magnetopause is assumed to be an ellipsoid of revolution (a prolate spheroid) as an approximation to observations (Sibeck et al., 1991). This assumption permits the potential γ to be expressed in spheroidal coordinates, expanded in spheroidal harmonics and its terms evaluated by performing inversion integrals. Finally, the field outside the magnetopause is replaced by zero, resulting in a consistent current closure along the magnetopause. This procedure can also be used to confine the modeled field of any other interior magnetic source, though the model current must always flow in closed circuits. The method is demonstrated on the T87 cross-tail current, examples illustrate the effect of changing the size and shape of the prescribed magnetopause and a comparison is made to an independent numerical scheme based on the Biot-Savart equation.

Introduction

Empirical models of the geomagnetic field are analytic expressions describing the average magnetosphere, satisfying Maxwell's equations and based on data. The magnetic field due to each source is usually represented separately, by an expression containing several free parameters, which are then fit to observations by least squares. In geospace, five principal magnetic field sources exist: the Earth's internal currents, the ring current, Birkeland currents, the cross-tail current and the magnetopause currents; each has its own unique character and so requires a distinct functional form to represent it.

This study is concerned with representing the field due to magnetopause currents. The empirical models of Tsyganenko (denoted here TU82, T87, and T89 for *Tsyganenko and Usmanov* [1982] and *Tsyganenko* [1987, 1989a], respectively) have used an exponential-polynomial representation for this component of the magnetic field, combinations of terms like $y^m z^n e^{x/\Delta x}$ (cos|sin)Ψ, where Ψ is the tilt angle of the Earth's dipole. Such all-purpose expansions were meant to represent not just the field of magnetopause currents, but also that of Birkeland currents and are likely to contain contributions from other sources as well.

One drawback of the polynomial expansion is that it is useful mainly in empirical global models fitted to data. If we want, for instance, to perform a "theoretical experiment" in which the tail current is doubled, we have no simple way to obtain a polynomial that will properly confine the new model field. Polynomials also do a poor job in representing Birkeland current fields, because such currents are relatively localized and polynomials do not represent small-scale features well.

Paper number 94JA01656.

A more serious deficiency is that the shape of the magnetopause in such models is indirectly determined by the interaction of polynomial terms with other sources, and hence may be irregular and hard to control. Note that the magnetopause in the TU82-T87-T89 models is actually a "de facto" surface defined by a bundle of field lines passing near the dayside null points. Since these models were based almost entirely on observations made well inside the boundary, this boundary should actually be considered to be an extrapolation. There may exist significant deviations of the de facto magnetopause from the real one, especially in poorly covered regions. Because of this, and also because of the inherent shortcomings of the polynomial representation, unrealistic magnetopause shapes appeared in some earlier models, especially for large tilt angles. This difficulty is avoided if the magnetopause shape is taken from observations of magnetopause crossings and is imposed on the model.

The field due to the magnetopause currents that confine the dipole field inside magnetopauses of simple symmetric shapes can be expressed by a scalar potential expanded in suitable harmonic functions [*Alexeev and Shabansky*, 1972; *Voigt*, 1972, 1981; *Stern*, 1985; *Tsyganenko*, 1989b]. This study continues the one by *Tsyganenko* [1989b], which assumed an ellipsoidal magnetopause shape, a convenient approximation to the observed magnetopause within the Moon's orbit [*Fairfield*, 1971; *Sibeck et al.*, 1991; *Roelof and Sibeck*, 1993]. The purpose of the present work is to extend this method to computing the field due to magnetopause currents that confine the field of any internal current system, in particular the cross-tail current.

Just as the dipole is the easiest source to confine inside a given magnetopause, since it is compact and symmetric, so the tail current is the most difficult one, because it extends to large distances in the antisunward direction and because its circuit closes on the magnetopause itself. Having successfully confined the tail field, we have no doubt that the same technique also

works with other internal fields, given appropriate models to represent them.

There exist other ways of deriving the magnetopause field confining the tail field, either by numerically deriving the scalar potential γ describing that field, as obtained by *Toffoletto et al.* [1994] or by a recursive application of the Biot-Savart integral, first used by *Mead and Beard* [1964]; in the appendix the latter method is used to further check our analytical approach. These methods allow any prescribed shape of the magnetopause to be used, but their output is numerical rather than analytical and therefore cannot well serve as a module in a data-based model. Neither is the model of *Schulz and McNab* [1987] suitable, since it uses a very simplified tail model.

Method

We assume that the boundary surface Σ is an ellipsoid of revolution (prolate spheroid) [*Tsyganenko* 1989b], approximating the directly observed magnetopause. We consider a fully closed magnetosphere, so that the magnetopause is the surface separating internal field lines from external ones. This separation is accomplished by an appropriate distribution of magnetopause currents, producing a magnetic field $\mathbf{B}_{MP}$ whose component normal to Σ cancels the normal component of the field $\mathbf{B}_{int}$ of interior sources

$$\mathbf{n}\cdot\mathbf{B}_{int} + \mathbf{n}\cdot\mathbf{B}_{MP} = 0 \qquad \text{on } \Sigma, \tag{1}$$

where $\mathbf{n}$ is the outward unit normal to Σ. Then, and only then, do no internal field lines cross Σ, and hence one might say that the tail field is confined to the magnetosphere or that the space outside Σ is "shielded" from internal field sources.

Provided the internal field $\mathbf{B}_{int}$ and the shape of the magnetopause Σ are known, it is possible (and convenient) to derive $\mathbf{B}_{MP}$ from the boundary condition (1). Under the assumption of a fixed ("prescribed") magnetopause shape, the boundary condition (1) is linear with respect to $\mathbf{B}_{MP}$ and $\mathbf{B}_{int}$; since $\mathbf{B}_{int}$ can be resolved into a sum of contributions from various internal sources (dipole, ring current etc.), $\mathbf{B}_{MP}$ too can be resolved into corresponding components, each of them shielding the field of one internal source and satisfying (1) with respect to its field.

When the various contributions to $\mathbf{B}_{int}$ are represented by parametric expressions and the corresponding parts of $\mathbf{B}_{MP}$ are added, their superposition gives a magnetospheric model that can then be fit to data. One can also perform theoretical experiments by specifying the internal currents and fields ad-hoc and superposing them and their shielding fields.

At this level we can distinguish two essentially different kinds of internal field sources. In the first case, the field to be shielded is produced by currents flowing entirely in the interior of the magnetosphere. The corresponding shielding currents form a completely separate circuit, confined to the magnetopause and forming there a two-dimensional surface current system. The contribution $\mathbf{B}_{MP}$ which they produce is therefore current-free in the interior and can be described there by a scalar potential γ:

$$\mathbf{B}_{MP} = -\nabla\gamma \qquad \nabla^2\gamma = 0 \tag{2}$$

The task of finding $\mathbf{B}_{MP}$ subject to (1), for this particular source, then reduces to a standard Neumann problem with the boundary condition [e.g., *Voigt*, 1972, 1981; *Stern*, 1985; *Tsyganenko*, 1990, and references therein]

$$\mathbf{n}\cdot\mathbf{B}_{int} + \mathbf{n}\cdot(-\nabla\gamma) = 0 \qquad \text{on } \Sigma \tag{3}$$

The second case is especially relevant to the cross-tail current and probably also to the Region 1 Birkeland currents. In this case the internal currents whose field is to be shielded extend to the magnetopause and include it in their circuit (Figure 1c). What should one take for $\mathbf{B}_{int}$ generated by such sources?

If the cross-tail current alone is viewed as the source of $\mathbf{B}_{int}$, we have an unclosed system with sources and sinks on the boundary, which means $\nabla\cdot\mathbf{J} \neq 0$ there. Furthermore, the magnetopause current is also unclosed, and for such systems [*Jackson*, 1975, eq. 5.21]

$$\nabla\times\mathbf{B} = \mu_0\mathbf{J} + \frac{\mu_0}{4\pi}\nabla\int d^3r' \frac{\nabla'\cdot\mathbf{J}(\mathbf{r}')}{|\mathbf{r}-\mathbf{r}'|} \tag{4}$$

Since the divergence of $\mathbf{J}$ appears in an integral, $\nabla\cdot\mathbf{J} \neq 0$ implies $\nabla\times\mathbf{B} \neq 0$ everywhere, even where $\mathbf{J} = 0$ locally, therefore the scalar potential cannot be used.

Some early models have actually used such truncated sheets [*Alexeev and Shabansky*, 1972; *Voigt*, 1972], but these representations are inconsistent, since they tacitly assumed that the equation $\nabla\times\mathbf{B} = 0$ holds separately for contributions from the equatorial current sheet and its closure/shielding complement. As discussed above, this is not true and hence, the direct use of scalar potentials is invalid.

Another approach, which goes back to the simplest model of *Williams and Mead* [1965] is to extend the cross-tail current outside the magnetosphere, in order to maintain current continuity, as shown in Figure 1a. A very useful by-product of this modification is that it allows the field components to be expressed in a simple analytic form, even for spread-out current sheets with finite thickness and current density variation in the tailward direction [*Tsyganenko and Usmanov*, 1982; *Tsyganenko*, 1987, 1989, *Stern*, 1990].

Let us denote as $\mathbf{B}_{tail}$ the field produced by the extended equatorial current sheet whose circuit is either closed or extends to infinity (Figure 1a). The central idea of the present work is to complement $\mathbf{B}_{tail}$ by a potential shielding field $\mathbf{B}_{MP} = -\nabla\gamma$, which satisfies everywhere on Σ the boundary condition (3), namely it cancels $\mathbf{n}\cdot\mathbf{B}_{tail}$, resulting in zero net normal component. The magnetopause currents are not considered explicitly at this stage; we only seek a scalar potential γ as a continuous function throughout space. Suppose we have found such a potential, ensuring that the net field is everywhere tangential to the boundary Σ. Now, we may replace the net field outside Σ with $\mathbf{B} = 0$, without violating Maxwell's equations [*Stern*, 1987, Figure 4]. (Moreover, instead of $\mathbf{B} = 0$ we could, in principle, replace the outside field with any other configuration $\mathbf{B}_{external}$, subject to only one restriction that $\mathbf{B}_{external}\cdot\mathbf{n} = 0$ on Σ; that would change the distribution of current on the magnetopause, but not the field inside, which is our main concern). As a result, the external part of the current sheet disappears and the internal current is rerouted (closed) via the magnetopause surface current (Figure 1c) with the density $\mathbf{K}$ implied by the discontinuity of the tangential component of $\mathbf{B}$ across Σ

$$\mu_0\mathbf{K} = -\mathbf{n}\times(\mathbf{B}_{tail} - \nabla\gamma) \tag{5}$$

Thus the desired solution is given by

$$\mathbf{B} = \mathbf{B}_{tail} - \nabla\gamma \qquad \text{inside } \Sigma \tag{6}$$

$$\mathbf{B} = 0 \qquad \text{outside } \Sigma$$

and satisfies all the requirements: $\mathbf{n}\cdot\mathbf{B} \equiv B_n = 0$ on Σ, the

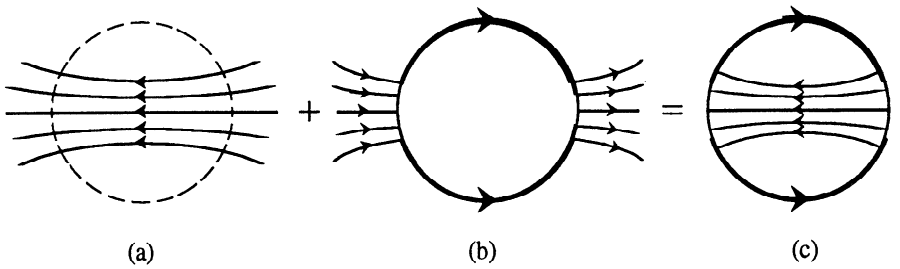

Figure 1. The superposition of the field due to the cross-tail current extended in some fashion so that is closes outside the magnetosphere (a), and the field produced by the current system (b) which is curl-free inside the magnetosphere, is equal to the magnetic field due to the desired net cross-tail–magnetopause current system (c).

divergence of the implied current is zero, the curl of **B** equals the actual cross-tail current inside, and is zero outside. In terms of electric currents, the procedure of the above described "equivalence decomposition" is illustrated in Figure 1: the extended current sheet (Figure 1a) providing the field $\mathbf{B}_{tail}$ is complemented by the current system of (Figure 1b), the field of which is curl-free inside the magnetosphere and hence can be represented there by $-\nabla\gamma$, to produce configuration (Figure 1c). Note, however, that the currents themselves do not enter the calculation, instead, we just find a potential γ satisfying the condition $B_n = 0$. Figure 1 only explains the logic of our approach in terms of current flow.

The modular approach, by which each internal source produces its own contribution $\mathbf{B}_{MP}$ to the magnetopause field, can also be adapted to the open magnetosphere. In that case, B_n on the magnetopause is not zero but has some specified distribution. In principle, the non-zero B_n can simply be added to the right-hand side of the boundary condition (3). However, it is more convenient to first perform the complete shielding of the tail and consider this as a zero-approximation model. After that, the effects of nonzero B_n can be taken into account by adding to the shielding field a current-free "interconnection field" [*Toffoletto and Hill*, 1989]

$$\mathbf{B}_{IF} = -\nabla\gamma_{IF} \qquad \nabla^2\gamma_{IF} = 0 \qquad (7)$$

subject to the boundary condition

$$B_n = -\mathbf{n}\cdot\nabla\gamma_{IF} \qquad \text{on } \Sigma.$$

Thus the possibility of an open configuration does not invalidate any of the preceding but merely adds another module. Of course, $\mathbf{B}_{IF}$ may affect force balance in the magnetosphere, and therefore the internal currents, for example, those of the tail [*Toffoletto and Hill*, 1989], may differ from those of the closed magnetosphere.

Ellipsoidal Boundary and Inversion Integral

We take the magnetopause as given by observations, specifically, as an ellipsoid fit to magnetopause crossings [*Sibeck et al.*, 1991]. We wish to solve Laplace's equation (2) with Neumann boundary conditions (3). Since our boundary is an ellipsoid, we use prolate spheroidal coordinates defined in terms of Cartesian coordinates by

$$\sigma = \frac{r_1 + r_2}{2a} \qquad \sigma \geq 1$$

$$\tau = \frac{r_1 - r_2}{2a} \qquad |\tau| \leq 1 \qquad (8)$$

$$\phi = \tan^{-1}(z/y)$$

where

$$r_1 = \sqrt{(x + x_0 + a)^2 + y^2 + z^2}$$

$$r_2 = \sqrt{(x + x_0 - a)^2 + y^2 + z^2}$$

Note that the origin has been shifted from the center of the ellipsoid to that of the Earth. Contours of constant σ and τ in the noon-midnight plane ($\phi = \pm\pi/2$) are shown in Figure 2.

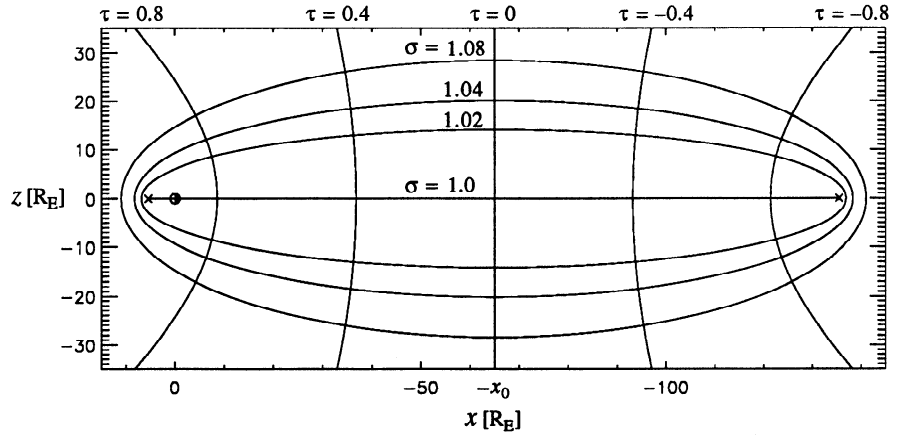

Figure 2. Prolate spheroidal coordinates, in which the surfaces of constant σ are ellipses and those of constant τ are hyperbolas. The Earth is located at $(x, z) = (0, 0)$ and the two foci shared by all ellipses and hyperbolas are marked with a cross. The x axis corresponds to σ=1 between the foci and to $\tau = \pm 1$ outside of that interval.

We use an ellipsoid fitted by *Sibeck et al.* [1991] for intermediate values of the solar wind dynamic pressure $P_{dyn} = nmv^2$, namely, 1.47 nPa < P_{dyn} < 2.60 nPa, characterized by the following parameters: magnetopause location

$$\sigma = \sigma_0 = 1.08$$

half-distance between foci

$$a = 70.5\ R_E$$

distance from the Earth to the near-Earth focus

$$d_{FE} = 5.48\ R_E$$

and distance from the Earth to the ellipsoid-center

$$x_0 = a - d_{FE} = 65.0\ R_E$$

Note the change in notation from *Tsyganenko* [1989b].

The general solution of Laplace's equation in this coordinate system is

$$\gamma = \sum_{n=1}^{\infty} \sum_{m=0}^{n} P_n^m(\sigma) P_n^m(\tau) \left(a_{nm} \cos m\phi + b_{nm} \sin m\phi\right) \quad (9)$$

where the P_n^m are associated Legendre functions. It must be noted that the different ranges for σ and τ, $\sigma \geq 1$, $|\tau| \leq 1$ require different choices of phase for the P_n^m [see *Abramowitz and Stegun*, 1964, section 8.3; *Morse and Feshbach*, 1953, p. 1286]. An inversion integral for the coefficients a_{nm} and b_{nm} can be obtained by substituting (9) into the boundary condition (3), multiplying by $P_n^m(\tau)$ and either cos $m\phi$ or sin $m\phi$ (for a_{nm} and b_{nm}

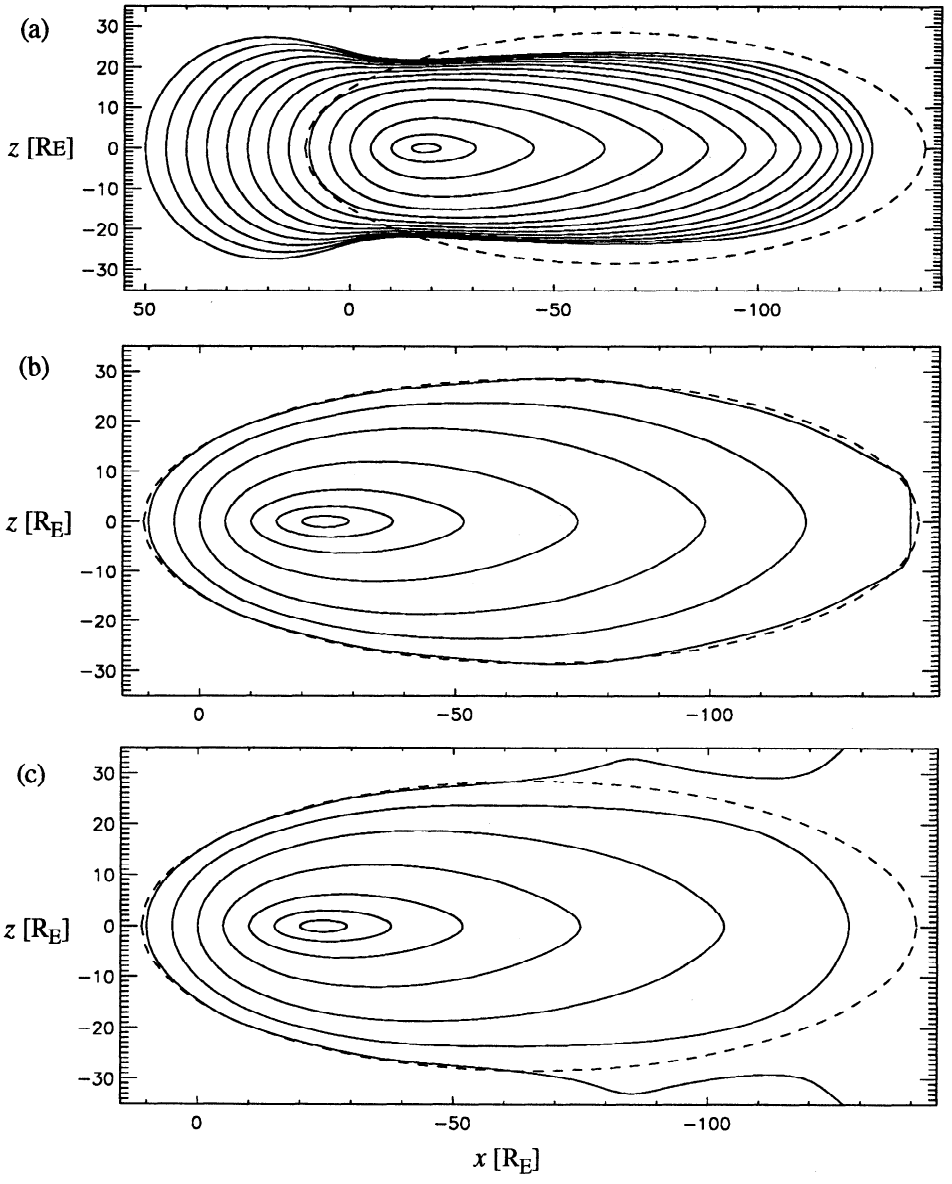

Figure 3. Field line plots in the noon-midnight meridian for the T87 cross-tail current for Kp = 0, 0$^+$, where the field is (a) unshielded, (b) shielded on the entire surface, and (c) shielded only on the sunward side of the ellipsoid. The dotted line is the desired magnetopause surface.

respectively), then integrating over the ellipsoid surface using the orthogonality of the Legendre and of trigonometric functions [*Tsyganenko*, 1989b] with the result

$$\begin{pmatrix} a_{n,m} \\ b_{n,m} \end{pmatrix} = \mathscr{A}_{nm} \int_{-1}^{1} d\tau \sqrt{\frac{\sigma^2-\tau^2}{\sigma^2-1}}\, P_n^m(\tau) \int_0^{2\pi} d\phi \begin{pmatrix} \cos m\phi \\ \sin m\phi \end{pmatrix} \hat{\mathbf{n}} \cdot \mathbf{B}_{\text{int}} \qquad (10)$$

where we define

$$\mathscr{A}_{nm} \equiv \frac{a}{\pi} \cdot \left[\frac{dP_n^m(\sigma)}{d\sigma} \right]_{\sigma=\sigma_0}^{-1} \times \begin{cases} \frac{1}{2} & m = 0 \\ 1 & m \neq 0 \end{cases}$$

We perform these integrations numerically. The integral over ϕ is performed first, using either Simpson's rule or Fehlberg integration (Fehlberg's method is preferred when the dipole tilt is not zero). The integral over τ is then performed using Simpson's rule.

The expansion for the confinement of a dipole was found by *Tsyganenko* [1989b]. For that case the inversion integral reduces to one dimension and only the a_{n0} and b_{n1} terms remain. To confine other internal sources, the full expansion may be necessary. As an illustration of the technique we shield here the original unwarped T87 cross-tail current for $Kp = 0, 0^+$.

The ellipsoid used here approximates the magnetopause for $x \gtrsim -40\ R_E$ [*Sibeck et al.*, 1991], that is, for only about 1/3 the length of the ellipsoid. Past $x = -40\ R_E$ this surface is not supported by observed magnetopause crossings but it does not contradict expectations until $x = -x_0 = -65.0\ R_E$ where the ellipsoid begins to narrow down again, in contrast with the actual magnetosphere, which maintains an approximately constant tail radius. For the confinement of the Earth's dipole [*Tsyganenko*, 1989b], that distant region has a negligible effect: the dipole field at those distances is very weak, and the added field needed to confine it there is negligible in comparison with the tail field which dominates that region. Thus, for shielding the Earth's dipole field, it does not matter if the confining surface is inaccurate in the far tail.

The tail current and field, on the other hand, persist to great distances. If the boundary condition is enforced along the entire ellipsoid, the field's behavior in the deep tail, where the ellipsoid closes, does not agree with observations. Figure 3a shows the unshielded field, while 3b gives field lines of a configuration completely shielded inside an ellipsoid, yielding a finite closed magnetosphere. In Figure 3 we include terms through m = 10 (120 terms, 30 of which are nonzero for the case of dipole tilt $\Psi = 0$).

It is also possible to shield the field only for $x > -x_0$ and leave B_n unchanged for $x < -x_0$, by matching $\partial\gamma/\partial n = 0$ tailward of x_0; the result is shown in Figure 3c. By comparing these extreme cases (Figures 3b and 3c) and others we have found that the boundary conditions deep in the tail have little effect on the field nearer the Earth. In particular, comparison of Figures 3b and 3c shows that the field lines in the region between the subsolar point and $x = -40$ are not visibly different. We also compare the fields produced by these two extreme cases numerically; in particular along the $y = z = 5\ R_E$ line between the subsolar point and $x = -40$, the largest difference occurs at $x = -40$, and is only about 0.5%, and even at $x = -60$ it is only about 2%. Therefore our results for $x \gtrsim -40\ R_E$ seem insensitive to the boundary condition at $x < -x_0$.

There is an independent method for computing the shielding magnetic field with good accuracy, based on a numerical procedure suggested by *Mead and Beard* [1964]. The method, based on the Biot-Savart equation, is a powerful tool for shielding fields within a wide class of boundaries. It was used in several earlier works for shielding Earth's dipole but is equally good for numerically solving the tail shielding problem. We provide a brief outline of this independent technique in the appendix and use it as a check on the results given by the scalar potential method. A comparison of results given by these two different methods shows good agreement.

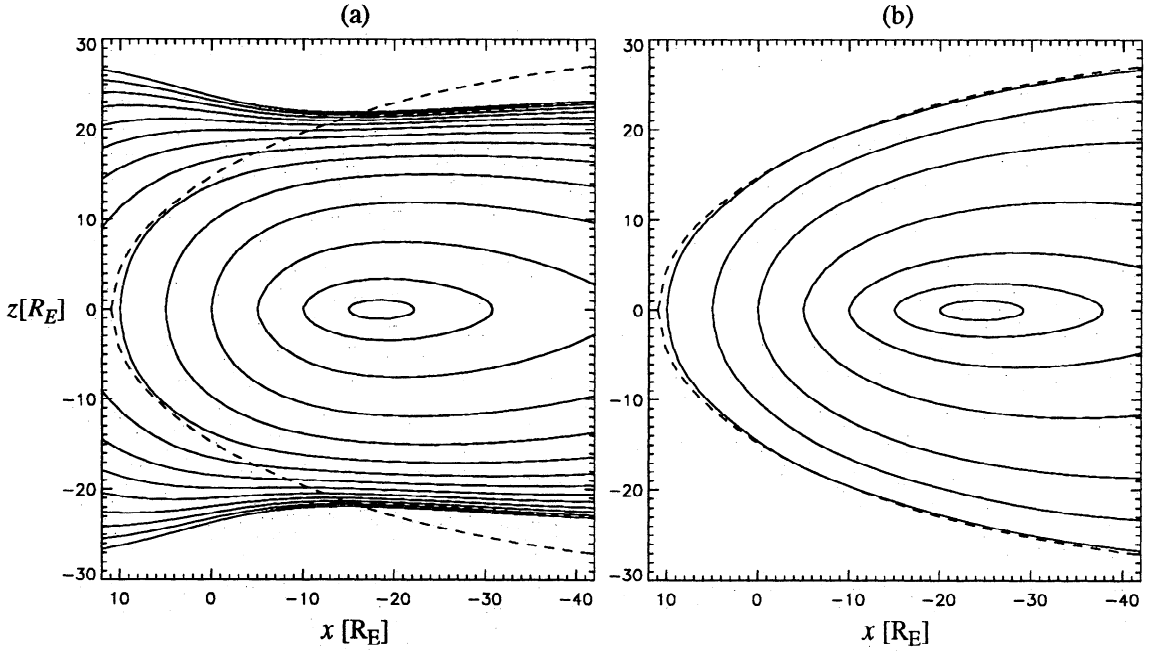

Figure 4. Field line plots for the T87 cross-tail current (a) without and (b) with shielding.

Results

Figure 4 again shows the magnetic field lines for the T87 cross-tail current, with and without shielding, magnified and

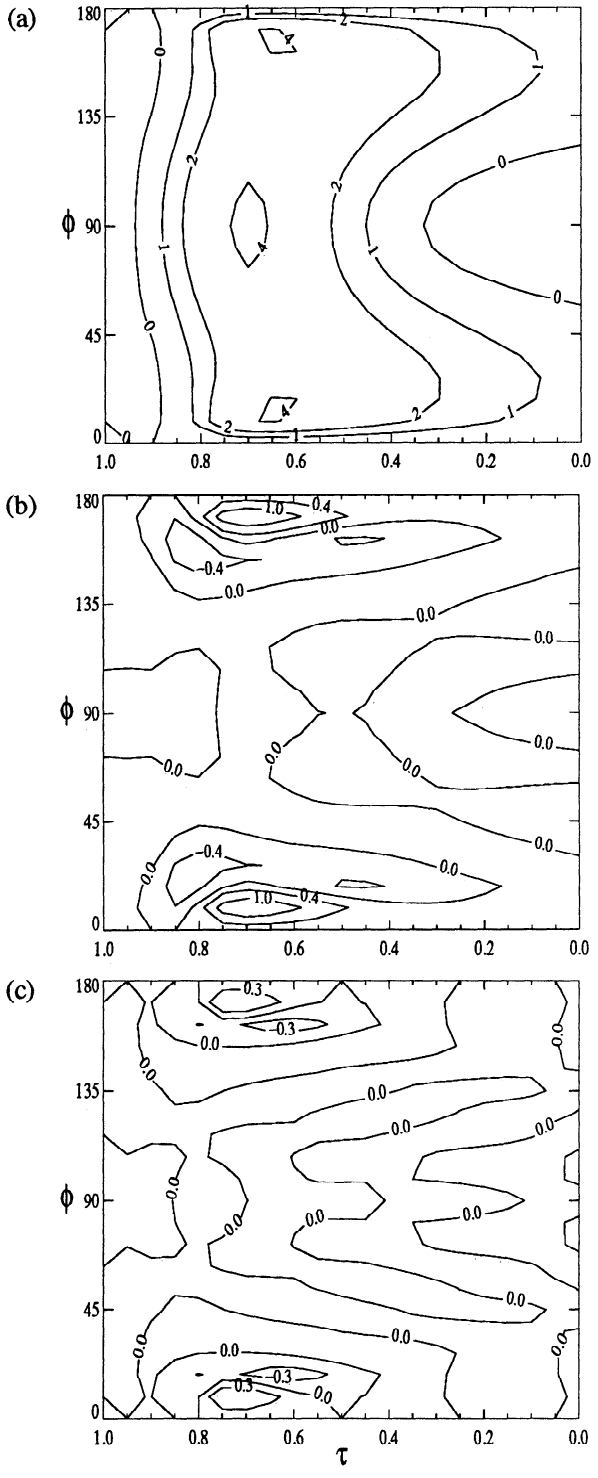

Figure 5. Contours of B_n (in nanotesla) on the magnetopause ($\sigma = \sigma_0 = 1.08$) as a function of the spheroidal coordinate τ and the rotation angle ϕ around the x axis ($\phi = 0$ in the $y>0$ equatorial plane) where (a) is without shielding, (b) is with shielding to order m=10 and (c) is with shielding to order m=15. The subsolar point corresponds to $\tau = 1$ (see Figure 2 and accompanying text for an explanation of spheroidal coordinates).

covering only the region in which the ellipsoidal surface is known to fit data. The expansion (9) of the shielding potential uses terms through m=10, corresponding to 120 terms, 30 of which are nonzero when the dipole tilt is zero. Figure 5 maps the distribution of the normal component of **B** (in nanotesla) on the entire upper half of the prescribed magnetopause, without shielding (Figure 5a) and with shielding (Figure 5b). It is clear that B_n has been greatly reduced on the entire surface. The residual B_n can be further reduced by adding terms to the shielding expansion, as shown in Figure 5c, where components up to m=15 (255 terms) have been used.

If we include the dipole field, tilted by 30°, and shield both the cross-tail current and the dipole, we obtain the field of Figure 6. In Figure 4b the outermost field line does not follow the magnetopause very well near the subsolar point, but the fit is much better in Figure 6, because in the subsolar region the dipole field is 5-10 times stronger than the tail field and its shielding is much more accurate.

For completeness, Figure 7 gives current flow lines on the magnetopause for the combined dipole-tail field (like the one in Figure 6, but here with Ψ=0) assuming no magnetic field outside the magnetopause. The flow lines are nested around the cusp, confirming quantitatively the pattern proposed by *Axford et al.* [1965]. The magnetopause current is found, for illustrative purposes only, using (5). This current system is calculated from the solution (6), not vice versa. Any magnetic field in the magnetosheath will, of course, modify this current system, but not the field inside.

When the T87 cross-tail current was fit to data, it was combined with a different magnetopause model, based on an exponential-polynomial expansion. Therefore it does not make much sense to discuss the accuracy of the resultant field in the present calculation. It is, however, instructive to study the effect of independently changing the magnetopause size and shape, keeping the cross-tail current fixed. We evaluate the effect of

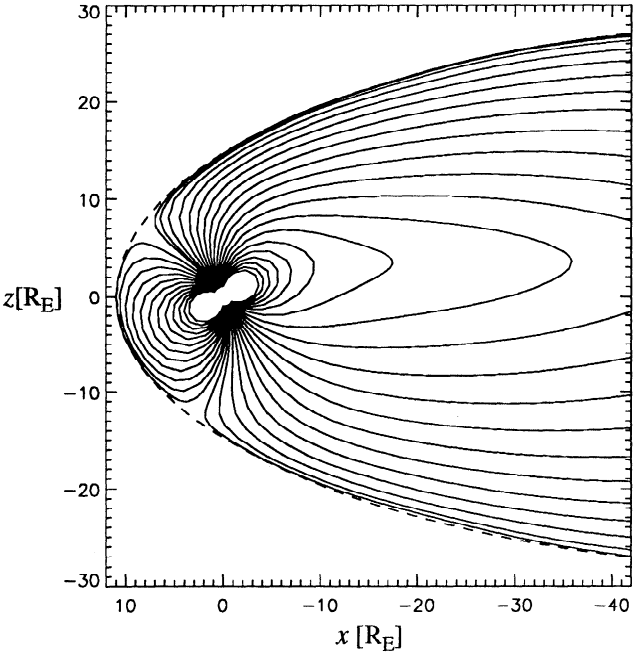

Figure 6. Field line plot of dipole and cross-tail current field with both sources shielded, the dipole tilted by $\Psi = 30°$ and the tail current sheet appropriately shifted.

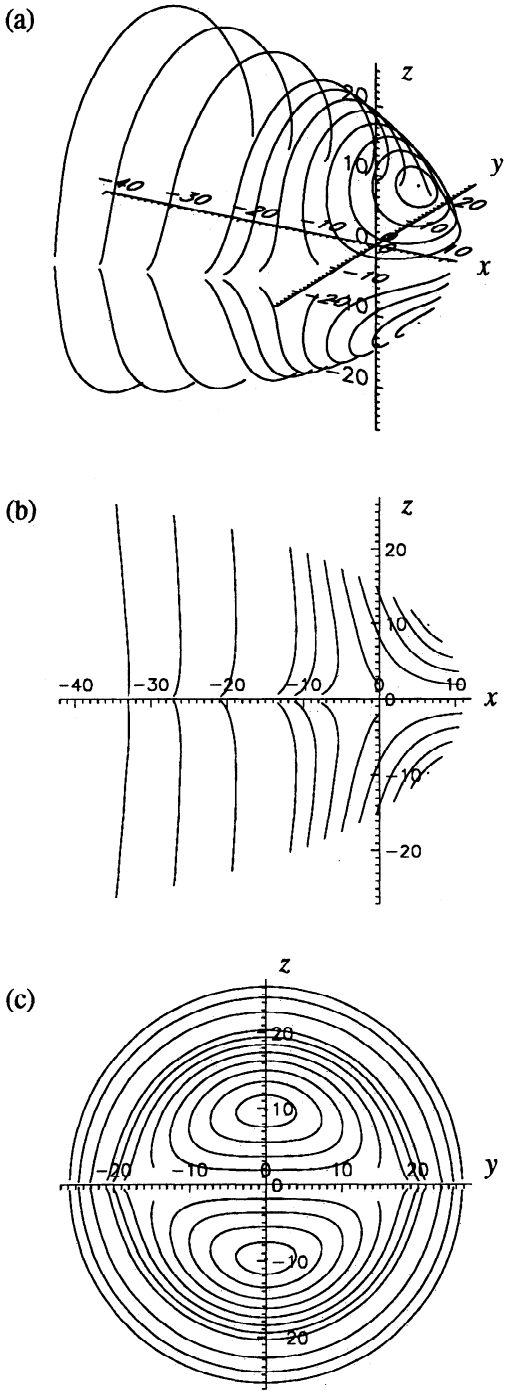

Figure 7. Current flow lines on the magnetopause: (a) as viewed from above the dawn flank, (b) projected onto the x-z plane and (c) projected onto the y-z plane.

these variations on the subsolar and geosynchronous magnetic fields and on the footpoint latitude of the polar cusp. Both the Earth's dipole and the cross-tail current are included as internal sources, the ring and Birkeland currents are not.

The magnetopause changes its size and shape in response to the changing solar wind. Changes in size are primarily an effect of changing solar wind dynamic pressure $P_{dyn} = n m v^2$, proportional to $P_{dyn}^{-1/6}$ [*Sibeck et al.*, 1991]. Changes in shape (i.e., flaring) are thought to result from the competing effects of dayside reconnection and nightside activity. Let pressure P_0 correspond to the ellipsoid fitted by *Sibeck et al.* [1991] for intermediate values 1.47 nPa < P_{dyn} < 2.60 nPa. Assuming here a self-similar variation, Table 1 compares the characteristic dimensions, the footpoint latitude of the cusp (defined in this context by the location of the magnetic field null point on the model magnetopause), noon geosynchronous field and subsolar field contributions for dynamic pressures $0.5P_0$, P_0, $2P_0$. The flaring angle of these three surfaces at $x = 0$ is 31.7° and we use the T87 cross-tail current for $Kp = [2^-, 2, 2^+]$.

The flaring angle, however, may vary independently, depending on the amount of magnetic flux in the tail, which itself is a function of the past history of magnetic reconnection. To model such variations, the same $Kp = [2^-, 2, 2^+]$ cross-tail current sheet is enclosed in three different magnetopauses of different flaring angle. The desired flaring angles are obtained by adjusting the average magnetopause while the subsolar distance and the distance to the ellipsoid center are kept fixed. The results appear in Table 2.

The footpoint latitude of the cusp seems to be strongly affected by the flaring angle, but not as much by changes in the solar wind dynamic pressure. The tabulated field strengths due to the shielded dipole are larger when the magnetopause is compressed and smaller for increased flaring, as expected. The tabulated field strengths due to the shielded cross-tail current are opposite to the dipole field in both direction and behavior. These estimates indicate general behavior but are limited in that one would not expect the cross-tail current to remain constant while the magnetopause changed shape and/or size and vice versa.

Summary

We have developed a method for obtaining the magnetopause field confining the tail field inside a prescribed ellipsoid of revolution, which gives a good approximation of the observed magnetopause [*Sibeck et al.*, 1991]. The field of any other internal source, for example, ring or Birkeland currents, may be confined by using the same method.

The model fields obtained here use the T87 tail current model of *Tsyganenko* [1987] and are meant only to illustrate the method. Examples demonstrate the effect of changing the size and shape of the prescribed magnetopause and a comparison to the numerical method of *Mead and Beard* [1964] is given in the appendix. In the future such tail-shielding expansions may be combined with a representation of the tail field as one of the modules in a global representation of the magnetospheric field, whose parameters are fit to data. Only then will the actual expansion terms become meaningful.

Appendix: Shielding Based on the Biot-Savart Equation—An Independent Test for the Scalar Potential Method

An independent method for computing the shielding magnetic field, based on a numerical procedure suggested by *Mead and Beard* [1964] that uses the Biot-Savart equation, is used to shield the T87 cross-tail current. The results are then compared to our previous analytic result.

An outline of this method is as follows. Consider a surface S enclosing an electric current system, some part of which may follow the surface as a boundary current. The problem is to find the distribution of shielding currents on the surface S, consistent with making $\mathbf{B} = 0$ in the exterior. Consider a point $\mathbf{r}$ inside S lying very close to the boundary. The total field at this point is

Table 1. Cusp latitude, Subsolar Field (Including Shielding Field) and Noontime Geosynchronous Field are Given for Different Size Magnetopauses Corresponding to Different Solar Wind Dynamic Pressures

Magnetopause					Geosynchronous Field			Subsolar Field		
SW Pressure	x_S	ρ_E	ρ_T	Cusp Latitude	Dipole	Tail	Total	Dipole	Tail	Total
$P = 0.5\ P_0$	12.4	16.5	31.9	78.1°	124.9	13.3	111.6	39.8	8.6	31.2
$P = P_0$	11.0	14.7	28.4	78.7°	133.8	12.3	121.5	56.3	8.5	47.7
$P = 2.0\ P_0$	9.8	13.1	25.3	79.1°	147.1	11.3	135.7	79.6	8.4	71.2

Subsolar distance (x_S), magnetopause radius at the Earth ($\rho = \rho_E$ at $x = 0$) and magnetopause radius in the tail ($\rho = \rho_E$ at $x = -65$) are given in R_E and magnetic field strengths are given in nanotesla.

$$\mathbf{B} = \mathbf{B}_{int} + \mathbf{B}_{MP} \tag{A1}$$

where $\mathbf{B}_{int}$ and $\mathbf{B}_{MP}$ are contributions from the internal part of the current system and from that lying at the boundary, respectively. The assumption of complete shielding of the magnetic field outside the boundary is equivalent to the statement that $\mathbf{B}$ is tangential to S and equals the jump in the field across the infinitely thin magnetopause. This yields an equation for the surface current density

$$\mu_0 \mathbf{K} \times \mathbf{n} = \mathbf{B}_{int} + \mathbf{B}_{MP} \tag{A2}$$

in which $\mathbf{n}$ is an inward unit normal to S and $\mathbf{B}_{MP}$ can be expressed as a Biot-Savart integral containing explicitly the surface current, thus reducing (A2) to an integral equation for $\mathbf{K}$, equivalent to that used by *Beard et al.* [1982]

$$\mathbf{K}(\mathbf{r}) = \mathbf{n} \times \left[\frac{\mathbf{B}_{int}}{\mu_0} + \frac{1}{4\pi} \int_S \frac{\mathbf{K}(\mathbf{r}') \times (\mathbf{r} - \mathbf{r}')}{|\mathbf{r} - \mathbf{r}'|^3} ds' \right] \tag{A3}$$

Following *Mead and Beard* [1964], we avoid problems with the singularity in the integrand by decomposing $\mathbf{B}_{MP}$ into a sum of two terms

$$\mathbf{B}_{MP} = \mathbf{B}_p + \mathbf{B}_c$$

where $\mathbf{B}_p$ is the contribution of a small area element ΔS in the immediate vicinity of $\mathbf{r}$ and $\mathbf{B}_c$ is the contribution of the rest of S. The singularity is confined to the vicinity of ΔS. Viewed from points infinitesimally close to the boundary, ΔS appears as an infinite plane, and therefore the local current density $\mathbf{K}(\mathbf{r})$ creates fields ($\mathbf{B}_p$, $-\mathbf{B}_p$) on opposite sides of the boundary. The other components $\mathbf{B}_{int}$ and $\mathbf{B}_c$ are continuous across the boundary, so just inside one gets

$$\mathbf{B}(\mathbf{r}) = \mathbf{B}_{int} + \mathbf{B}_c + \mathbf{B}_p$$

and just outside

$$0 = \mathbf{B}_{int} + \mathbf{B}_c - \mathbf{B}_p$$

Adding the two equations, we have

$$\mathbf{B}(\mathbf{r}) = 2(\mathbf{B}_{int} + \mathbf{B}_c) \tag{A4}$$

Since

$$\mathbf{B}_c = \frac{\mu_0}{4\pi} \int_{S-\Delta S} \frac{\mathbf{K}(\mathbf{r}') \times (\mathbf{r} - \mathbf{r}')}{|\mathbf{r} - \mathbf{r}'|^3} ds' \tag{A5}$$

we get from (A4) and from $\mu_0 \mathbf{K}(\mathbf{r}) = \mathbf{n} \times \mathbf{B}(\mathbf{r})$

$$\mathbf{K}(\mathbf{r}) = \mathbf{n} \times \left[\frac{2}{\mu_0} \mathbf{B}_{int} + \frac{1}{2\pi} \int_{S-\Delta S} \frac{\mathbf{K}(\mathbf{r}') \times (\mathbf{r} - \mathbf{r}')}{|\mathbf{r} - \mathbf{r}'|^3} ds' \right] \tag{A6}$$

This may be viewed as a recursion for obtaining $\mathbf{K}(\mathbf{r})$, starting from $\mathbf{K} = 0$ on the right. This equation was used by *Tsyganenko* [1976, 1981] for shielding the magnetospheric field in earlier models. It is a powerful method, applicable for any shape of the shielding surface; however, it has a disadvantage: the final solution of (A6) is only available numerically in the form of large arrays of the electric current components. Nonetheless, it is a good tool for testing our analytic solutions; results of such a test are described below.

Table 2. Cusp Latitude, Subsolar Field (Including Shielding Field) and Noontime Geosynchronous Field are Given for Different Flaring Angles (at $x = 0$)

Magnetopause					Geosynchronous Field			Subsolar Field		
Flare	x_S	ρ_E	ρ_T	Cusp Latitude	Dipole	Tail	Total	Dipole	Tail	Total
28°	11.0	12.7	24.5	80.4°	140.5	10.0	130.5	57.7	6.4	51.3
31.7°	11.0	14.7	28.4	78.7°	133.8	12.3	121.5	56.3	8.5	47.7
35°	11.0	16.7	32.2	77.3°	129.4	14.4	115.0	55.2	10.7	44.5

Subsolar distance (x_S), magnetopause radius at the Earth ($\rho = \rho_E$ at $x = 0$) and magnetopause radius in the tail ($\rho = \rho_T$ at $x = -65$) are given in R_E and magnetic field strengths are given in nanotesla.

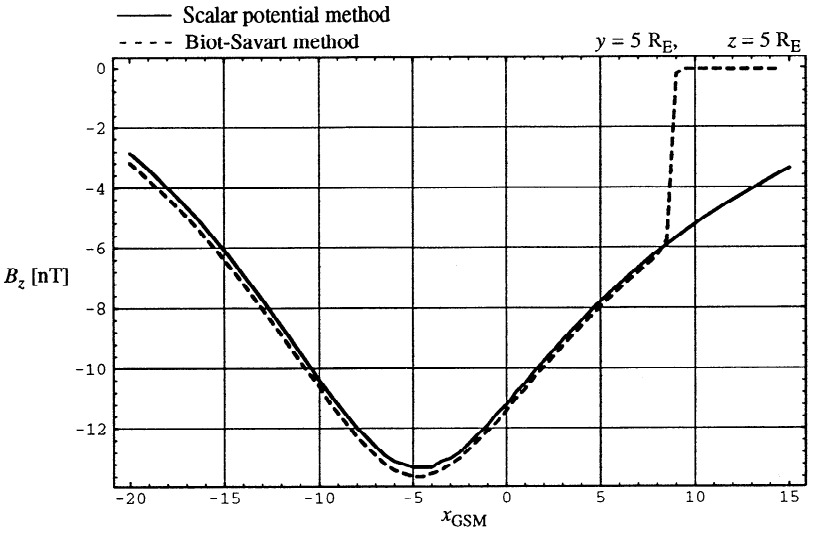

Figure 8. The net B_z at $y = z = 5\,R_E$ as a function of x for the shielded Kp = [0⁻, 0, 0⁺] T87 cross-tail current is plotted using both potential and Biot-Savart shielding for purposes of comparison.

We chose the integration surface S to be the same ellipsoid Σ as was used in finding our analytic solution. The internal field $\mathbf{B}_{\text{int}}$ is that produced by the T87 current sheet; however, an important difference between this numerical method and the analytical scheme is that the field $\mathbf{B}_{\text{int}}$ in (A6) is only the contribution of the part of the T87 current sheet lying inside the magnetosphere (hence computed numerically), while in computing the expansion coefficients (10) we used analytical formulas giving the field of the full T87 current, which extends to infinity outside the magnetopause. The ellipsoid boundary was divided into 1971 elements comprising a non-uniform mesh, covering the surface from the subsolar point up to $x = -77\,R_E$ in the tail. Magnetopause currents were evaluated by solving (A6) iteratively; for each iteration, the components of $\mathbf{K}$ at the center of each element were found by summing over the remaining elements. The iterations converged quickly, 8-10 cycles were quite sufficient to obtain a self-consistent solution.

Figure 8 shows a profile of the z component of the numerically computed field of a shielded current sheet along a line parallel to the x axis, compared with the corresponding result given by the analytical solution (6). The difference between the two plots is negligible, becoming significant only outside the model magnetosphere, where the numerical solution abruptly goes to zero, as it should, while the harmonic expansion yields a continuous extension of the internal solution to the outside. As already noted, since the shielding procedure ensures zero normal component at the boundary, we can set $\mathbf{B} = 0$ outside the ellipsoidal cavity.

Acknowledgments. This work was performed while two of us (N.A.T. and T.S.) held National Research Council-NASA Goddard Space Flight Center Research Associateships.

The Editor thanks R. V. Hilmer and another referee for their assistance in evaluating this paper.

References

Abramowitz, M., and I.A. Stegun, *Handbook of Mathematical Functions*, National Bureau of Standards, Gaithersburg, Md., 1964.

Alexeev, I.I., and V.P. Shabansky, A model of the magnetic field in the geomagnetosphere, *Planet. Space Sci., 20*, 117, 1972.

Axford, W.I., H.E. Petschek, and G.L. Siscoe, Tail of the magnetosphere, *J. Geophys. Res., 70*, 1231, 1965.

Beard, D.B., D. Hirschi, and K. Propp, The tailward magnetopause field beyond 10 R_E, *J. Geophys. Res., 87*, 2533, 1982.

Fairfield, D.H., Average and unusual locations of the Earth's magnetopause and bow shock, *J. Geophys. Res., 76*, 6700, 1971.

Jackson, J.D., *Classical Electrodynamics, 2nd ed.*, John Wiley, New York, 1975.

Mead, G.D., and D.B. Beard, Shape of the geomagnetic field solar wind boundary, *J. Geophys. Res., 69*, 1169, 1964.

Morse, P.M., and H. Feshbach, *Methods of Theoretical Physics*, McGraw-Hill, New York, 1953.

Roelof, E.C., and D.G. Sibeck, The magnetopause shape as a bivariate function of the solar wind ram pressure and IMF B_Z, *J. Geophys. Res., 98*, 21,421, 1993.

Schulz, M., and M.C. McNab, Source-surface model of the magnetosphere, *Geophys. Res. Lett., 14*, 182, 1987.

Sibeck, D.G., R.E. Lopez, and E.C. Roelof, Solar wind control of the magnetopause shape, location and motion, *J. Geophys. Res., 96*, 5489, 1991.

Stern, D.P., Parabolic harmonics in magnetospheric modeling: The main dipole and the ring current, *J. Geophys. Res., 90*, 10,851, 1985.

Stern, D.P., Tail modeling in a stretched magnetosphere, 1, Methods and transformations, *J. Geophys. Res., 92*, 4437, 1987.

Stern, D.P., A model of the magnetospheric tail with current free lobes, *Planet. Space Sci., 38*, 255, 1990.

Toffoletto, F.R., and T.W. Hill, Mapping of the solar wind electric field to the Earth's polar caps, *J. Geophys. Res., 84*, 329, 1989.

Toffoletto, F.R., et al., Solution of the Chapman-Ferraro problem with an arbitrary magnetopause, *Geophys. Res. Lett., 21*, 621, 1994.

Tsyganenko, N.A., A model of the cislunar magnetospheric field, *Ann. Geophys., 32*, 1, 1976.

Tsyganenko, N.A., Numerical models of quiet and disturbed geomagnetic field in the cislunar part of the magnetosphere, *Ann. Geophys., 37*, 381, 1981.

Tsyganenko, N.A., Global quantitative models of the geomagnetic field in the cislunar magnetosphere for different disturbance levels, *Planet. Space Sci., 35*, 1347, 1987.

Tsyganenko, N.A., A magnetospheric magnetic field model with a warped tail current sheet, *Planet. Space Sci., 37*, 5, 1989a.

Tsyganenko, N.A., A solution of the Chapman-Ferraro problem for an ellipsoidal magnetopause, *Planet. Space Sci., 37*, 1037, 1989b

Tsyganenko, N.A., Quantitative models of the magnetospheric magnetic field: Methods and results, *Space Sci. Rev., 54*, 75, 1990.

Tsyganenko, N.A., and A. Usmanov, Determination of the magnetospheric current system parameters and development of experimental geomagnetic field models based on data from IMP and HEOS satellites, *Planet. Space Sci.*, *30*, 985, 1982.

Voigt, G.-H., A three dimensional analytical magnetospheric model with defined magnetopause, *Z. Geophys.*, *38*, 319, 1972.

Voigt, G.-H., A mathematical magnetospheric field model with independent physical parameters, *Planet. Space Sci.*, *29*, 1, 1981.

Williams, J., and G.D. Mead, Nightside magnetospheric configuration as obtained from trapped electrons at 1100 kilometers, *J. Geophys. Res.*, *70*, 3017, 1965.

T. Sotirelis, D. P. Stern, and N. A. Tsyganenko, Laboratory for Extraterrestrial Physics, NASA Goddard Space Flight Center, Greenbelt, MD 20771. (email: xr2ts@lepvax.gsfc.nasa.gov; u5dps@lepvax.gsfc.nasa.gov; ys2nt@lepvax.gsfc.nasa.gov)

(Received November 15, 1993; revised June 15, 1994; accepted June 21, 1994)